Supplemental Figures

Figure S1

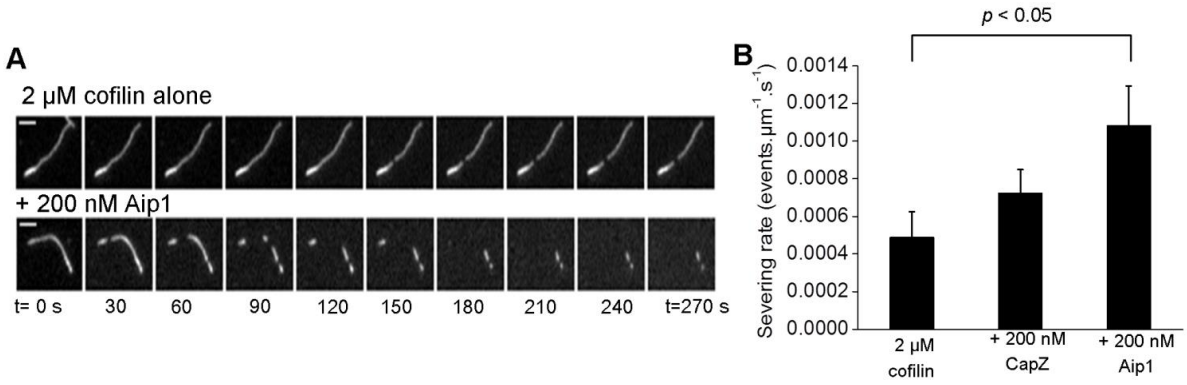

Figure S2

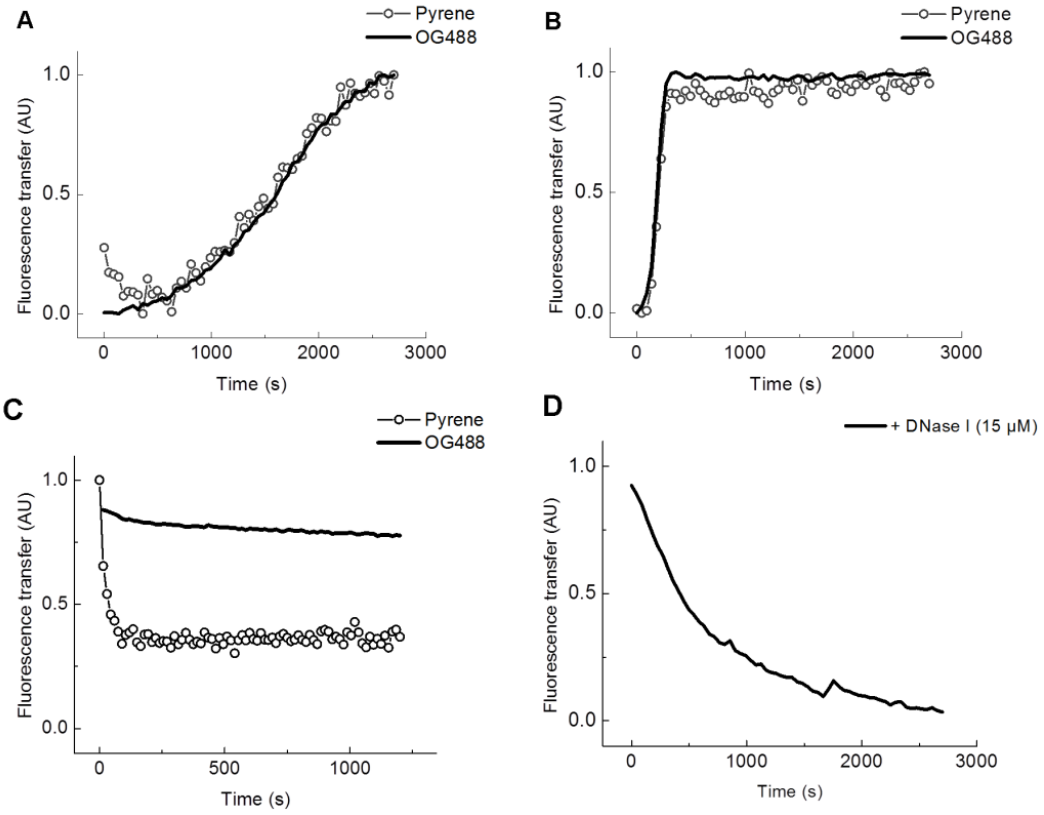
A
Pyrene
OG488
Fluorescence transfer (AU)
Time (s)
B
Pyrene
OG488
Fluorescence transfer (AU)
Time (s)
C
Pyrene
OG488
Fluorescence transfer (AU)
Time (s)
D
+ DNase I (15 μM)
Fluorescence transfer (AU)
Time (s)

Figure S3

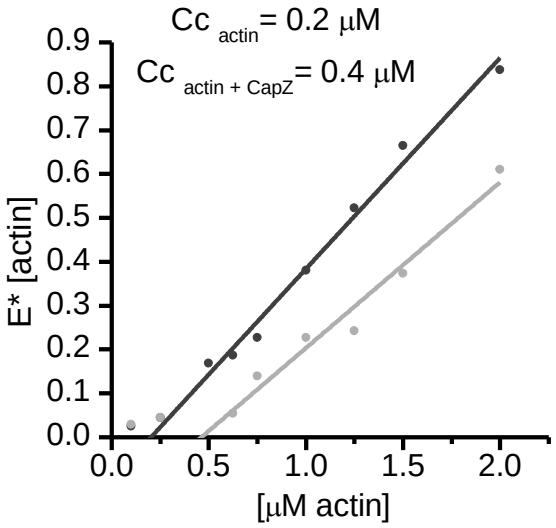
Cc actin = 0.2 μM
Cc actin + CapZ = 0.4 μM
E* [actin]
[μM actin]
0.0
0.1
0.2
0.3
0.4
0.5
0.6
0.7
0.8
0.9
0.0
0.5
1.0
1.5
2.0

Supplemental Figure Legends

Figure S1: Aip1 but not CapZ increases cofilin-mediated severing rates

(A) Frames from a time lapse movie showing severing of polarity marked filaments in the presence of cofilin alone and cofilin + Aip1. **(B)** Quantitation of rates from n=3 movies shows that the increase in the severing rate is statistically significant in the presence of Aip1 and not CapZ. Scale bars represent 1 µm, error bars represent S.D., p=0.159. This relates to Figure 4 in the main paper.

Figure S2: FRET assay reports on kinetics of actin assembly. (A) Polymerization of 3.5 µM actin measured by FRET (black line) and pyrene (gray circles). (B) Addition of Arp2/3 (500 nM) and ActA (200 nM) significantly reduces the lag phase of both the pyrene and FRET signals. Normalized fluorescence transfer is plotted against time. Representative kinetic data from n=3 experiments is shown. (C) At pH 6.7, cofilin binds to F-actin and quenches pyrene fluorescence (gray open circles) whereas the FRET signal is not significantly changed indicating there is little depolymerization (black line). (D) The assay reports on polymer loss. DNase I (15 µM) depolymerizes all F-actin to monomer, as reported by decrease in FRET down to 0. This relates to figure 5.

Figure S3 The FRET assay was used to measure actin critical concentration. (A) Oregon green fluorescence intensity was measured in solutions containing increasing concentrations but a constant ratio of red to green actin (roughly 3:1). The point at which assembly of actin is observed is denoted as the critical concentration, which is 0.2 µM in the case of F-actin alone (black line). The addition of 0.1 µM CapZ increases the critical concentration as it caps the barbed end to 0.4 µM (gray line). This relates to Figure 5 in the main paper.

Supplemental Experimental Procedures:

Antibodies: Cofilin antibodies were raised in-house to recombinant cofilin and secondary antibodies (anti HRP-rabbit) were purchased from Zymed.

Protein purification: Actin was purified as previously described [S1] and gel filtered on a Sephacryl S-300 (GE-Healthcare) column. Recombinant human cofilin-1 was purified as previously described [S2] with modifications. Briefly, cofilin was expressed in *E.coli* BL21 cells by IPTG induction. The supernatant of the lysed bacterial cells was passed over a DE-52 column (Whatman) equilibrated in 20 mM TRIS pH 8.0, 50 mM NaCl, 1 mM EDTA and 1 mM PMSF (Buffer A). Cofilin was contained in the flowthrough and relevant fractions were passed over a Q-column (GE Healthcare) equilibrated in Buffer A. Cofilin, contained in the flow-through, was purified by ultracentrifugal concentration and gel filtration on a Sephacryl S-300 column. Aip1 was purified using the same series of ion exchange, hydrophobic interaction and gel filtration columns as described previously [S2]. ActA [S3] , Arp2/3 [S4], CapZ [S5] and filamin [S6] were purified as previously described.

Preparation of thymus extract: Thymus was homogenized in 1:1 buffer (20 mM TRIS pH 7.4, 20 mM KCl, 5 mM $MgCl_2$, 2 mM EGTA, 1 mM PMSF) with a standard blender, and spun at 10,500 x g for 30 min. The supernatant was spun at 150,000xg for 90 minutes. The supernatant from this was used for depolymerization assays.

Fluorescent labeling of actin: Pyrene-actin and Oregon Green 488 actin were prepared as described [S7]. Briefly, G-actin was labeled on cysteines with a stoichiometric amount of N-pyrene or Oregon Green 488 (Molecular Probes, Invitrogen). Actin was immediately polymerized by addition of 100 mM KCl, 2 mM $MgCl_2$ and 0.5

mM ATP. The reaction was allowed to proceed overnight at room temperature (N-Pyrene maleimide) or at 4ºC (Oregon Green 488 maleimide). Filaments were collected by centrifugation at 140,500 X g for 2 hours, resuspended in G-buffer, and dialyzed exhaustively against G-Buffer (containing DTT). G-Actin was subsequently gel filtered on a Sephacryl S- 300 column (GE Healthcare). Pyrene actin was 80% labeled and Oregon Green actin was 60-80% labeled. 80% TMR-actin was prepared as described [S8]. Alexa-647 actin was prepared as described [S9].

Development of FRET: The copolymerization of Oregon green (OG) and tetramethylrhodamine (TMR) actin leads to increased fluorescent energy transfer and consequent quenching of donor (OG) actin fluorescence over time. The FRET assay has been used in the past to report on the kinetics of actin assembly [S10, S11], and we confirmed these results by examining the kinetics of actin polymerization of a mixture of green and red actin with a small amount of pyrene actin added as a tracer. Aliquots of labeled actin were diluted to 20 µM in G buffer (pH 7.4) and spun the next day at 227,900 X g for 20 minutes. 35-40% Tetramethylrhodamine labelled actin and 12-15% Oregon green 488 labelled actin were premixed at 20 µM. For polymerization assays (200 µl in a 96-well plate), polymerization was initiated by diluting G- actin 3 µM in 1x F-buffer(10 mM HEPES 7.8, 50 mM KCl, 0.5 mM EGTA, 1 mM $MgCl_2$, 1 mM ATP). To monitor assembly, 0.5 µM 80% labeled spun pyrene-actin was added to the reaction as a tracer. Total actin in the reaction was 3.5 µM. Excitation wavelengths for Pyrene and OG488 were 365 nm and 490 nm respectively. Fluorescence intensity was detected at 410 nm and 530 nm on a Spectramax M2 fluorimeter (Molecular Devices).

The kinetics of actin assembly as measured by the FRET signal matched that of the pyrene signal. The addition of actin nucleators, *Listeria monocytogenes* surface protein 200 nM ActA and 500 nM Arp2/3 reduced the lag phase of both the pyrene signal and the FRET signal when added during the assembly phase.

Cofilin binds but cannot disassemble F-actin actin at acidic pH [S12, S13]. We took advantage of this property to test whether the FRET signal was insensitive to cofilin binding. The FRET signal was undisturbed by the addition of 2 μM cofilin to 3.5 μM F-actin at steady state at pH 6.7. In contrast the pyrene signal was quenched by cofilin binding to F-actin at this pH. The FRET signal does decay, however, when polymer mass is lost following addition of DNaseI which sequesters actin monomers [S14]. DnaseI was added from a stock to a final concentration of 15 uM after the actin had reached steady state.

Imaging of actin single filaments: Perfusion chambers were assembled as previously described using pre-cleaned coverslips [S9]. Single filament imaging was carried out in two ways. For figures 1,2 and 3, the actin filaments were suspended in solution to saturate filaments as attachment of actin to coverslips with filamin or alpha-actinin induced severing at higher concentrations of cofilin due to competition for cofilin-binding. 3.75 μM monomeric Alexa-647 actin was pre-polymerized for 90 seconds and perfused into chambers coated with 200 nM CapZ (to ensure retention of actin in the chamber) and blocked with casein. The buffer used was 10 mM HEPES pH 7.8, 50 mM KCl, 1 mM $MgCl_2$, 0.5 mM EGTA and 1 mM ATP (1x F-buffer). The chamber was washed gently with 2 volumes of 1xF-buffer and imaged in 1xF-buffer supplemented with 4.5 mg/ml glucose, 0.2 mg/ml glucose oxidase and 2 mM Trolox (1xPhotobuffer).

Photobuffer was freshly prepared every 2 hours. Filaments were imaged on an Axioimager M1 microscope with a 63X 1.4 N.A. objective (Zeiss). Images were acquired by a Hamamatsu Orca-ER camera with 2x2 binning on Axiovision software.

In experiments with saturating amounts of cofilin, filaments were always pre-saturated by addition of 25 µM cofilin in the presence of 0.5% methylcellulose in 1X Photo-Buffer. After this, varying concentrations of Aip1 were perfused in the presence of saturating cofilin and severing events were enumerated as the number of visual breaks per second normalized to the amount of polymer measured in microns.

For the experiments where we varied the concentration of Aip1 and cofilin keeping the other constant, the depolymerizers were flowed in at the same time in 1xPhoto-Buffer.

For the experiments where we measured depolymerization rates at ends, coverslips were coated with 80 µg/ml filamin (in 1xF-buffer) and subsequently blocked with casein for 10 minutes. Filaments were polarity marked by initially polymerizing 50% labeled Alexa-647 actin at 5 µM for 20 seconds in a 3 µl volume. Seeds were then diluted 10 –fold, and allowed to grow for 90 seconds in the presence of 1.8 µM 20% labeled Alexa 547-monomeric actin in the perfusion chamber as described. Kymographs were generated using Fiji software. Rates were quantitated as slope of the kymograph, and converted into number of subunits per second.

Elongation of polymerized Oregon green actin filaments was carried out in the presence of 2 µM monomeric Alexa 647 actin, 150 nM cofilin and 200 nM of either CapZ or Aip1 for 60 seconds. This was compared to a control with actin alone.

Supplemental References:

S1. Pardee, J. D., and Spudich, J. A. (1982). Purification of muscle actin. Methods Enzymol. *85 Pt B*, 164–81.

S2. Brieher, W. M., Kueh, H. Y., Ballif, B. A., and Mitchison, T. J. (2006). Rapid actin monomer–insensitive depolymerization of Listeria actin comet tails by cofilin, coronin, and Aip1. J. Cell Biol. *175*, 315–324.

S3. Skoble, J., Portnoy, D. A., and Welch, M. D. (2000). Three regions within ActA promote Arp2/3 complex-mediated actin nucleation and Listeria monocytogenes motility. J. Cell Biol. *150*, 527–538.

S4. Higgs, H. N., Blanchoin, L., and Pollard, T. D. (1999). Influence of the C terminus of Wiskott-Aldrich syndrome protein (WASp) and the Arp2/3 complex on actin polymerization. Biochemistry *38*, 15212–15222.

S5. Soeno, Y., Abe, H., Kimura, S., Maruyama, K., and Obinata, T. (1998). Generation of functional beta-actinin (CapZ) in an E. coli expression system. J. Muscle Res. Cell Motil. *19*, 639–46.

S6. Shizuta, Y., Shizuta, H., Gallo, M., Davies, P., and Pastan, I. (1976). Purification and properties of filamin, and actin binding protein from chicken gizzard. J. Biol. Chem. *251*, 6562–7.

S7. Bryan, J., and Coluccio, L. M. (1985). Kinetic analysis of F-actin depolymerization in the presence of platelet gelsolin and gelsolin-actin complexes. J. Cell Biol. *101*, 1236–1244.

S8. Tang, V. W., and Brieher, W. M. (2012). Actinin-4/FSGS1 is required for Arp2/3-dependent actin assembly at the adherens junction. J. Cell Biol. *196*, 115–30.

S9. Kueh, H. Y., Charras, G. T., Mitchison, T. J., and Brieher, W. M. (2008). Actin disassembly by cofilin, coronin, and Aip1 occurs in bursts and is inhibited by barbed-end cappers. J. Cell Biol. *182*, 341–353.

S10. Taylor, D. L., Reidler, J., Spudich, J. A., and Stryer, L. (1981). Detection of actin assembly by fluorescence energy transfer. J. Cell Biol. *89*, 362–367.

S11. Wang, Y. L., and Taylor, D. L. (1981). Probing the dynamic equilibrium of actin polymerization by fluorescence energy transfer. Cell *27*, 429–436.

S12. McGough, a, Pope, B., Chiu, W., and Weeds, a (1997). Cofilin changes the twist of F-actin: implications for actin filament dynamics and cellular function. J. Cell Biol. *138*, 771–81.

S13. Pope, B. J., Gonsior, S. M., Yeoh, S., McGough, A., and Weeds, A. G. (2000). Uncoupling actin filament fragmentation by cofilin from increased subunit turnover. J. Mol. Biol. *298*, 649–661.

S14. Hitchcock, S. E. (1980). Actin deoxyroboncuclease I interaction. Depolymerization and nucleotide exchange. J. Biol. Chem. *255*, 5668–5673.